IEEE Access
Multidisciplinary | Rapid Review | Open Access Journal

Received April 1, 2020, accepted April 26, 2020, date of publication April 29, 2020, date of current version May 14, 2020.

Digital Object Identifier 10.1109/ACCESS.2020.2991158

Design of a Circularly-Polarized UHF Antenna for Partial Discharge Detection

SEUNGYONG PARK AND KYUNG-YOUNG JUNG, (Senior Member, IEEE)
Department of Electronics and Computer Engineering, Hanyang University, Seoul 04763, South Korea

Corresponding author: Kyung-Young Jung (kyjung3@hanyang.ac.kr)

This work was supported by the Institute of Information and Communications Technology Planning and Evaluation (IITP) Grant funded by the Korea Government (MSIT) (Advanced and integrated software development for electromagnetic analysis) under Grant 2019-0-00098.

ABSTRACT In this work, a circularly-polarized ultra-high frequency (UHF) partial discharge (PD) antenna is proposed to detect the PD in 0.6 GHz – 1.7 GHz. The proposed PD antenna consists of an Archimedean spiral antenna, a balun, and a cavity. The Archimedean spiral antenna is embedded by FR-4 as substrate and superstrate for miniaturization. The microstrip-to-paired strips balun is designed to yield good performance in the return loss, insertion loss, and amplitude and phase imbalances which are of great necessity for low axial ratio. The cavity is employed to obtain unidirectional radiation patterns and prevent external signal interference. However, it is found that the originally-designed cavity-backed antenna does not work properly near 1.35 GHz due to resonance phenomena in the cavity. In this work, the cavity is modified to tackle this problem. The proposed UHF PD antenna is fabricated and measured and the results show that it provides good impedance matching, realized gain, radiation pattern, and circular polarization.

INDEX TERMS Broadband antennas, partial discharges, UHF antennas.

I. INTRODUCTION

When the localized electric field strength in high-voltage equipment is larger than the breakdown electric field strength of a dielectric, the partial discharge (PD) may happen. Repeated PDs may result in destroying high-voltage power equipment. Therefore, diagnosing PDs is of great importance to maintain high-voltage power equipment. PD events are accompanied with physical phenomena such as electromagnetic (EM) wave radiation, acoustic pressure, chemical reaction, etc. Until now, various PD detection methods have been developed by measuring physical phenomena. The ultra-high frequency (UHF) method based on the utilization of EM waves is one of the most promising methods since it can provide PD localization and online monitoring. The PD antenna for the UHF method can be primarily classified as an external sensor and an internal sensor and it is employed in transformers, gas-insulated switchgears, wind power devices, power cables, etc. The external sensor and the internal sensor are determined by the installing location of the PD antenna. In contrast with the external sensor, the internal sensor has several main advantage such as high signal-to-noise ratio, high sensitivity, and anti-interference [1]–[4].

The associate editor coordinating the review of this manuscript and approving it for publication was Lu Guo.

The favorable performances of the UHF PD antenna include broadband characteristic and unidirectional radiation pattern. In addition, circular polarization is highly desirable since it is robust in multipath environment such as high-voltage power equipment [5]–[7]. A cavity-backed spiral antenna is widely utilized for PD detection sensors because a spiral antenna can have broadband and circular polarization characteristics and a cavity can provide unidirectional radiation patterns and simultaneously prevent external signal interference. Recently, some researchers studied spiral-type antennas for PD detection [8]–[14]. Various cavity-backed spiral antennas were studied by using inductors [8], resistors [9], a ring-shaped absorber [10], or bow-tie loading [11]. In addition, a spiral antenna was proposed to reduce its size by employing sine-wave meandered arms [12] and an equiangular spiral antenna with a horizontal balun was proposed for easy package [13]. A single-arm spiral antenna directly fed by a coaxial cable was also proposed in [14]. Although circular polarization performance is significantly important, the axial ratio of the PD antennas was not presented to clarify the circular polarization performance [8]–[13] or the PD antenna does not satisfy the axial ratio less than 3 dB in the frequency of interest [14]. A stand-alone spiral antenna is usually circularly polarized but a cavity-backed spiral PD antenna may not provide circular polarization characteristic

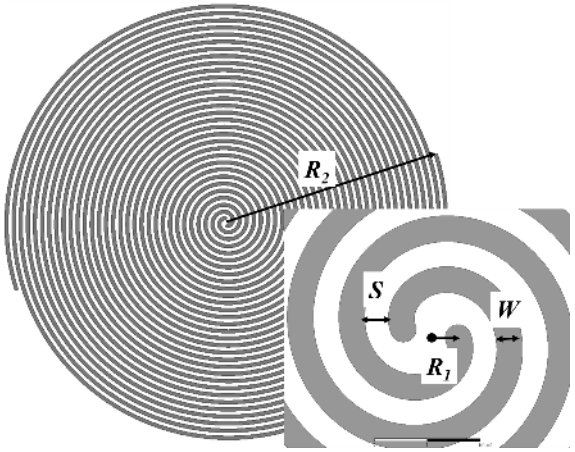

FIGURE 1. Archimedean spiral antenna.

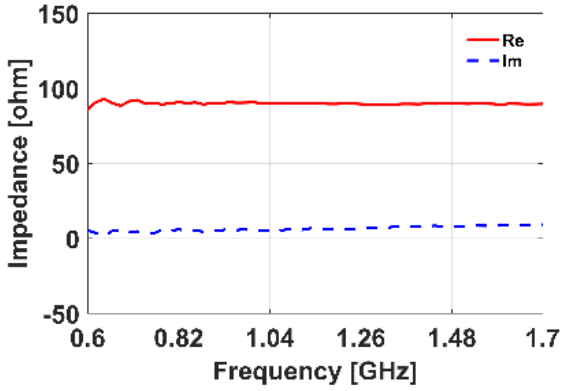

FIGURE 2. Simulated input impedance of the Archimedean spiral antenna.

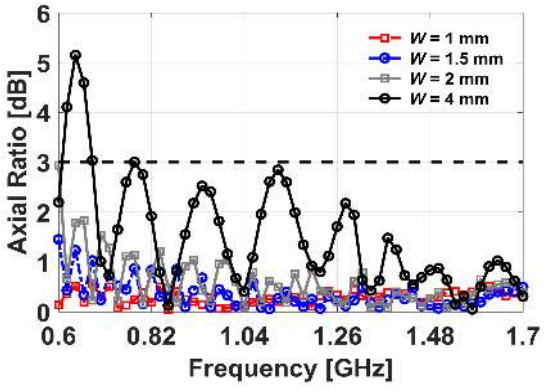

FIGURE 3. Simulated axial ratio of the Archimedean spiral antenna for various *W*.

because its performance is determined by not only the spiral antenna but also both cavity and balun. For example, it is found that the axial ratio for the UHF PD antenna in [14] is larger than 3 dB in 2 GHz – 2.2 GHz although a spiral antenna was employed. Therefore, it is of great necessity to design a circularly-polarized UHF PD antenna by considering the performance of the spiral antenna with a cavity and a balun.

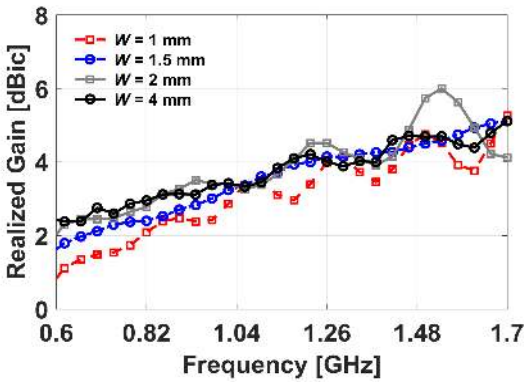

FIGURE 4. Simulated realized gain of the Archimedean spiral antenna for various *W*.

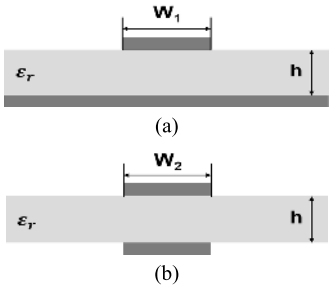

FIGURE 5. Microstrip line and paired strips. (a) Microstrip line. (b) Paired strips.

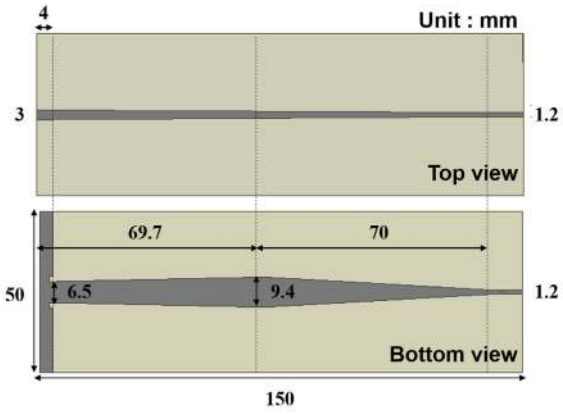

FIGURE 6. Top and bottom views of the designed balun.

In this work, we propose a circularly-polarized UHF PD antenna in the frequency range from 0.6 GHz to 1.7 GHz. The designed UHF PD antenna consists of an Archimedean spiral antenna, a balun, and a cavity. The Archimedean spiral antenna is employed since it can provide broadband and circular polarization characteristics. The balun is made of microstrip line for the single-ended SMA connector and paired strips for the differential input of the Archimedean spiral antenna. The cavity is utilized to provide unidirectional radiation pattern and prevent external signal interference. However, we found that the originally-designed UHF PD

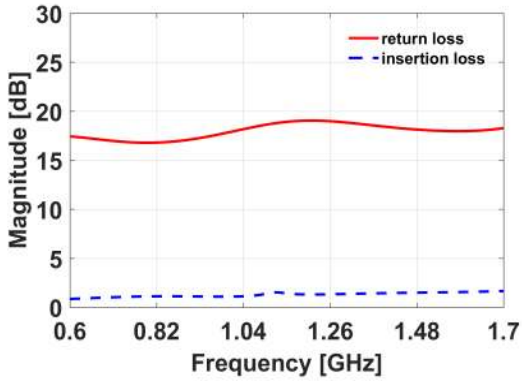

FIGURE 7. Simulated return loss of the matched balun and insertion loss of the back-to-back balun.

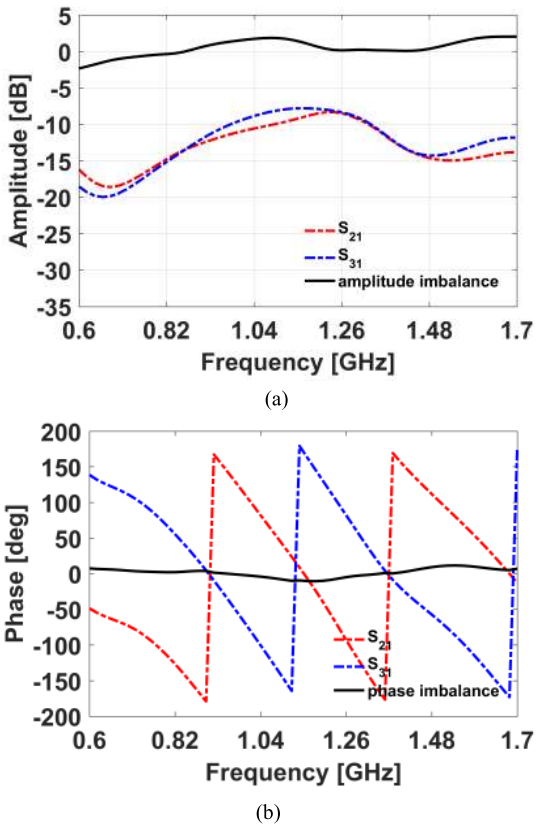

FIGURE 8. Simulated amplitude and phase imbalances of the balun. (a) Amplitude imbalance. (b) Phase imbalance.

antenna does not operate as a radiator near 1.35 GHz. To tackle this problem, the cavity is modified and the resulting UHF PD antenna yields good performance in the frequency range of interest. The remainder of this paper is organized as follows. We first present the design of the two-arm Archimedean spiral antenna and the balun. Next, we investigate performance of the original cavity-backed UHF PD and then propose the modified cavity-backed UHF PD antenna to eliminate the cavity resonance problem. Experimental results of the fabricated circularly-polarized

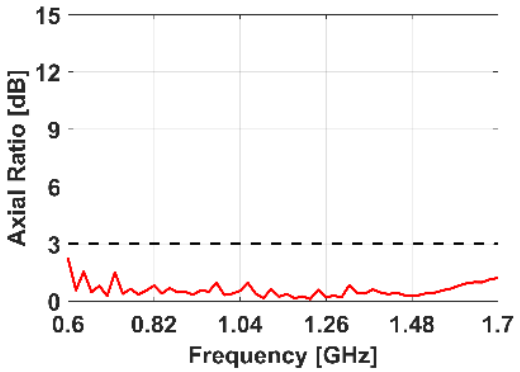

FIGURE 9. Simulated axial ratio of the Archimedean spiral antenna connected with the balun.

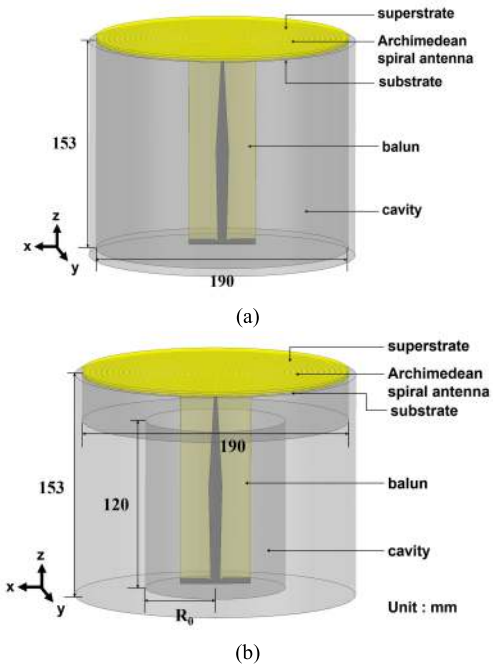

FIGURE 10. Scheme of designed PD antenna. (a) Original PD antenna. (b) Modified PD antenna.

UHF PD antenna are presented. Finally, concluding remarks are provided.

II. DESIGN

A. ARCHIMEDEAN SPIRAL ANTENNA

In the Archimedean spiral antenna, the width W is equal to the spacing S due to the self-complementary structure [15]. The input impedance of the Archimedean spiral antenna is ideally 188 Ω [16]. However, the input impedance of the practical Archimedean spiral antenna is lower than 188 Ω because of its finite size. The designed Archimedean spiral antenna is shown in Fig. 1. In theory, when the curve drawn by the antenna arm is one-wavelength circumference, the Archimedean spiral antenna can radiate at the corresponding frequency. Note that the lower the operating frequency, the larger antenna size. For the purpose of decreasing the size

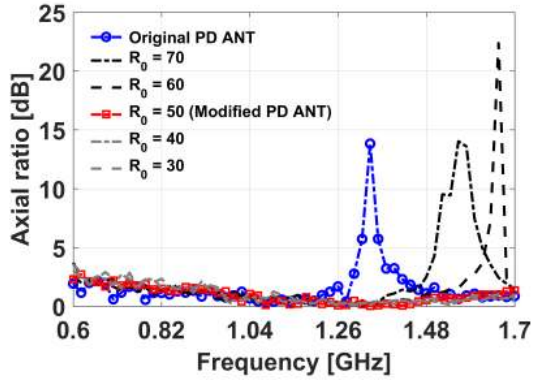

(a)

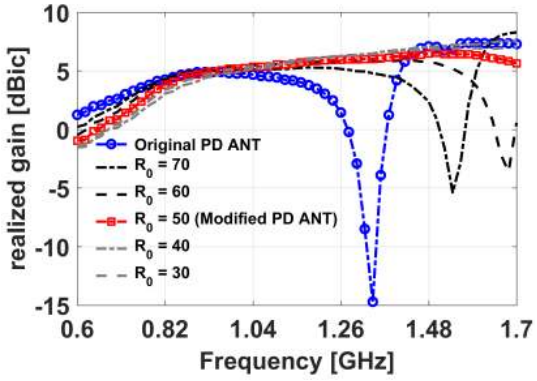

(b)

FIGURE 11. Simulated realized gain results of the designed PD antenna. (a) Axial ratio. (b) Realized gain.

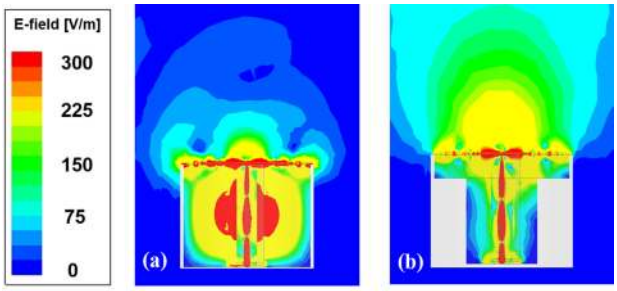

FIGURE 12. Electric field distribution at 1.35 GHz. (a) Original PD antenna. (b) Modified PD antenna.

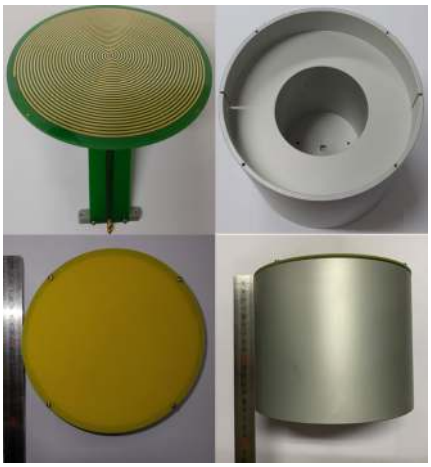

(a)

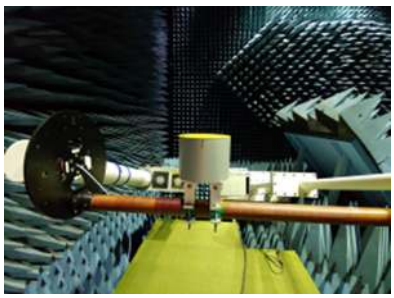

(b)

FIGURE 13. Fabrication and measurement setup of PD antenna. (a) Fabrication. (b) Measurement setup.

and input impedance of the antenna, the antenna is embedded between substrate and superstrate, which are FR-4 (thickness $= 1.6$ mm, $\varepsilon_r = 4.4$, $\tan\delta = 0.02$) [17]. Note that high input impedance of the Archimedean spiral antenna makes it difficult to fabricate a balun since the width of paired strips in the balun should be extremely narrow.

In the Archimedean spiral antenna design, to determine its overall size, the antenna size is gradually increased until the input impedance of the antenna embedded by superstrate and substrate is almost constant in the frequency of interest. The maximum radius R_2 of the antenna is 93 mm, which leads to the input impedance of almost constant 90 Ω as shown in Fig. 2. The width of the antenna should be properly determined since it affects the axial ratio and the realized gain of the antenna, especially for lower operating frequencies. The axial ratio and the realized gain are depicted in Figs. 3 and 4. From Fig. 3, it is observed that W should be less than 2 mm to marginally have an axial ratio less than 3 dB. Note that it turns out that $W = 2$ mm leads to the axial ratio of 4 dB at 0.6 GHz when the spiral antenna is connected with a balun and a cavity. According to Fig. 4, the realized gain is low at lower operating frequencies for $W = 1$ mm. Therefore, in this work, W is chosen as 1.5 mm. The number of turns N by an antenna arm is determined in [14]. In this work, the turns N is 15.3 and the minimum radius R_1 is 0.8 mm.

B. BALUN

The input port of the Archimedean spiral antenna is fed by a differential feed line whereas an SMA connector is inherently single-ended. To match the input port of the Archimedean spiral antenna with the SMA connector, the balun should be employed. The balun is made of microstrip line (for matching the single-ended 50 Ω SMA connector) and paired strips (for the differential 90 Ω input of the antenna). The width W_1 of a microstrip line for a given 50 Ω characteristic impedance ($Z_{C,M}$) and the width W_2 of paired strips for a given 90 Ω characteristic impedance ($Z_{C,P}$) in Fig. 5 can be obtained well-known formulation [18]. In this work, a FR-4 dielectric substrate with the thickness of 1.6 mm is used in the microstrip-to-paired strips balun. It is found that the width W_1 of 3 mm and the width W_2 of 1.2 mm lead to the desired characteristic impedances. Note that the width of the

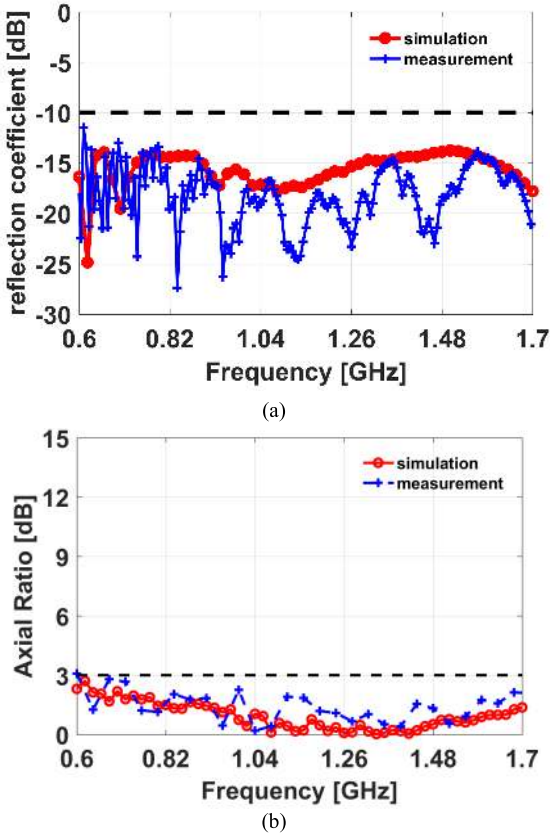

FIGURE 14. Reflection coefficient and axial ratio of the proposed PD antenna. (a) Reflection coefficient. (b) Axial ratio.

FR-4 substrate is chosen as 50 mm in order for the balun to be robustly attached to the antenna. Note that the taper function of the balun is linear and the geometrical parameters of the transition region in the balun is optimized to have good performance. Figure 6 shows the top and the bottom views of the designed balun.

The performance evaluation of the balun is performed by the methodology employed in [19]. The return loss is larger than 10 dB and the insertion loss is less than 3 dB as shown in Figure 7. The amplitude and phase imbalances can be obtained by a three-port network as in [19]. Figure 8 (a) and (b) show the results of the amplitude and phase differences between S_{21} and S_{31}. Note that port 1 indicates the differential input of the balun and port 2 and port 3 indicate the other two output ports. It is observed that the amplitude and phase imbalances are low in the frequency range of interest. Figure 9 shows the simulated axial ratio for the Archimedean spiral antenna connected with the designed balun. As shown in the figure, it is observed that the axial ratio of is less than 3 dB in the frequency of interest.

C. UHF PD ANTENNA

As alluded previously, the cavity should be employed in PD detection to prevent external noise interference. The cavity material is aluminum and the diameter of the inner cavity is 190 mm, which is equal to the superstrate and substrate

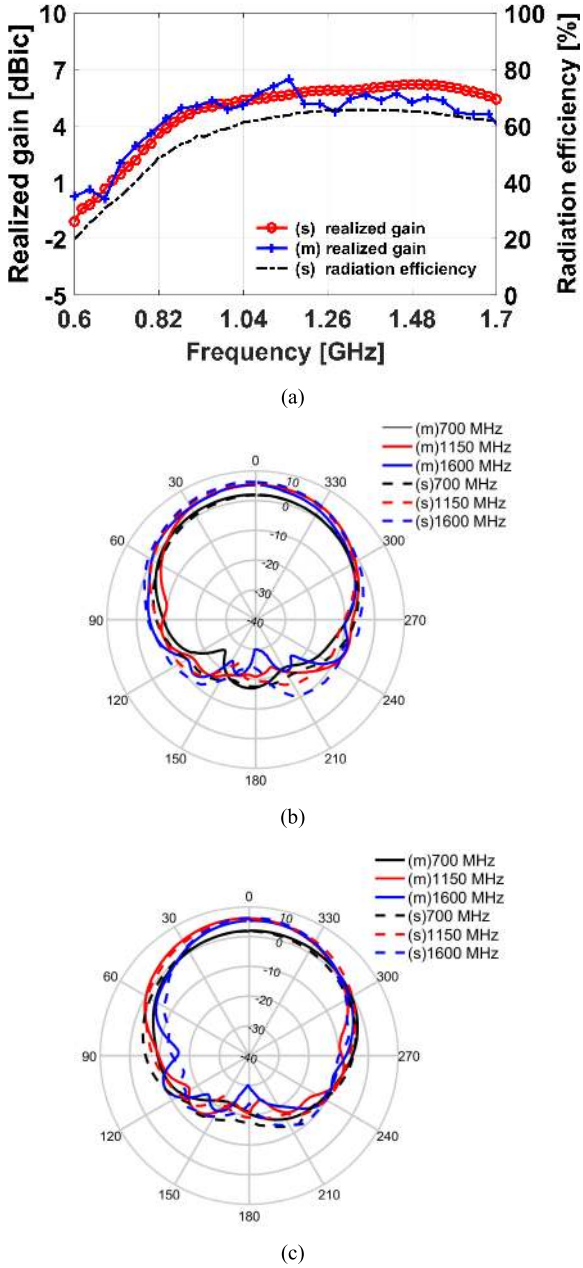

FIGURE 15. Realized gain, radiation efficiency, and radiation patterns of the fabricated proposed PD antenna. (a) Realized gain and radiation efficiency. (b) Radiation patterns in the xz plane. (c) Radiation patterns in the yz plane. Measurement and simulation results are indicated in (m) and (s) respectively.

of the Archimedean spiral antenna. The height of the cavity is 153 mm. The schematic of the originally-designed PD antenna is depicted in Fig. 10 (a). Figure 11 presents the simulated results of the axial ratio and the realized gain for the original PD antenna. The results imply that the original PD antenna does not work as a radiator at 1.35 GHz. In other words, the original PD antenna may operate as a resonator at 1.35 GHz. To investigate how the original PD antenna operates at 1.35 GHz, we examine electric field distribution at

TABLE 1. Comparison of spiral-type PD antennas.

Ref.	-10 dB S_{11} Bandwidth (GHz)	Antenna Diameter (mm)	Antenna Substrate	Measured Realized Gain (dBic)	Radiation Pattern	3dB Axial Ratio Bandwidth (GHz)
This work	0.6 – 1.7	200	FR-4	0.3 @ f_{min} / 4.6 @ f_{max}	Unidirectional	0.6 – 1.7
[8]	1.15 – 2.4	212.1 [a]	FR-4	-1 @ f_{min} / 8 @ f_{max}	Unidirectional	Not presented
[9]	0.925 – 1.6	95	FR-4	6 @ f_c	Unidirectional	Not presented
[10]	0.5 – 1.5	192	TLY-5A	3 @ f_{min} / 7.5 @ f_{max}	Unidirectional	Not presented
[11]	1 – 3	132	Not presented	2.5 @ f_{min} / 11.7 @ f_{max}	Unidirectional	Not presented
[12]	0.92 - 3	95.2	FR-4	1.4 @ f_{min} / 5.1 @ f_{max}	Bidirectional	Not presented
[13]	0.7 – 3	218	Not presented	Not presented	Bidirectional	Not presented
[14]	1.2 – 2.4	95.6	FR-4	Not presented	Bidirectional	0.6 – 2.0

[a]Diagonal length of the antenna.

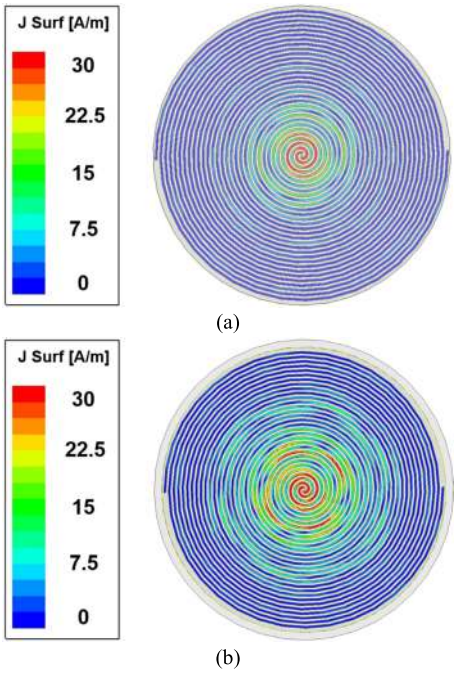

FIGURE 16. Current distribution at 1600 MHz (a) Archimedean spiral antenna (b) Proposed PD antenna consisting of the Archimedean spiral antenna, the balun and the cavity.

the corresponding frequency. As shown in Fig. 12 (a), electric fields are significantly stored inside the cavity, which infers that it works as a resonator rather than a radiator. In addition, to support our claim, the eigenmode analysis of the original PD antenna is performed by using the eigenmode solver in HFSS. It is found that the eigenfrequency for a high quality factor is 1.35 GHz due to the cavity resonance.

To eliminate unwanted cavity resonance phenomena at 1.35 GHz, in this work, the cavity is modified by reducing the cavity volume as shown in Fig. 10 (b). Note that the radius of the cavity just below the Archimedean spiral antenna is not changed such that it cannot significantly affect the Archimedean spiral antenna. Figure 11 shows the simulated results of the axial ratio and the realized gain with respect to the radius (R_0) of the modified cavity. As the radius decreases, the cavity resonance frequency increases due to larger cavity. It is also found that the eigenfrequency is shifted to higher as the radius decreases from the eigenmode analysis. As depicted in Fig. 11, when the radius is below 50 mm, the PD antenna performance is good in the frequency of interest, without cavity resonance phenomena. In this work, the radius of 50 mm is chosen to save fabrication cost of the cavity. We also investigate electric field distribution of the modified PD antenna in Fig. 12 (b). As shown in the figure, the modified PD antenna operates as a radiator rather than a resonator, different from the original PD antenna.

III. FABRICATION AND MEASUREMENT

The designed circularly-polarized PD antenna is fabricated and measured in Fig. 13. The simulated and measured results of the reflection coefficient and the axial ratio for the proposed PD antenna are shown in Fig. 14. The measurement results are generally in agreement with the simulation results. Discrepancies between the measurement results and simulation results may be caused by the fabrication errors (of the spiral antenna, the balun, and the cavity) and measurement errors. The measured reflection coefficient of the fabricated PD antenna is below -10 dB from 0.6 GHz to 1.7 GHz depicted in Fig. 14 (a) and the good axial ratio is observed in Fig. 14 (b). The measured realized gain is larger than 0 dBic in the frequency range of interest as shown in Fig. 15 (a). The radiation patterns at various frequencies are also shown in Fig. 15 (b) and (c). Unidirectional radiation patterns can be observed. It is also observed that radiation pattern tends to be tilted at the high frequency. The proposed PD antenna consists of not only the Archimedean spiral

antenna but also the balun and the cavity. Therefore, the current distribution of the proposed PD antenna is different from that of the Archimedean spiral antenna. We plot the current distribution for the stand-alone Archimedean spiral antenna and the proposed PD antenna in Fig. 16 (a) and Fig. 16 (b) respectively. As shown in the figure, the current distribution of the proposed PD antenna is different from the stand-alone Archimedean spiral. That is why the radiation pattern is little bit tilted. Finally, Table 1 shows the comparison between the proposed PD antenna and the previous spiral-type PD antennas. Some PD antennas yield bidirectional radiation patterns since a cavity was not employed and thus they are vulnerable to external signal interference. As shown in the table, the proposed PD antenna can present unidirectional radiation patterns and circular polarization simultaneously in the frequency range of interest.

IV. CONCLUSION

In this paper, a circularly-polarized PD antenna is proposed to detect UHF PD signals in a high-voltage power equipment. The PD antenna is designed on the basis of a two-arm Archimedean spiral antenna, which is embedded between FR-4 substrate and superstrate. The microstrip-to-paired strips balun is employed to match the single-ended SMA connector to the differential input of the two-arm Archimedean spiral antenna. The antenna is covered with a cavity to have unidirectional radiation pattern and to protect external noise interference. However, when the spiral antenna covered by the original cavity, the antenna does not operate properly at 1.35 GHz because of resonance phenomena in the cavity. To avoid the cavity resonance, the modified cavity is proposed. The proposed PD antenna is fabricated and measured. Experimental results demonstrate that the proposed PD antenna has good performance in impedance matching, realized gain, radiation pattern, and circular polarization and thus it is suitable for PD detection systems.

REFERENCES

[1] S.-G. Ha, J. Cho, J. Lee, B.-W. Min, J. Choi, and K.-Y. Jung, "Numerical study of estimating the arrival time of UHF signals for partial discharge localization in a power transformer," *J. Electromagn. Eng. Sci.*, vol. 18, no. 2, pp. 94–100, Apr. 2018.
[2] M. D. Judd, L. Yang, and I. B. B. Hunter, "Partial discharge monitoring of power transformers using UHF sensors. Part I: Sensors and signal interpretation," *IEEE Elect. Insul. Mag.*, vol. 21, no. 2, pp. 5–14, Mar. 2005.
[3] H. Chai, B. T. Phung, and S. Mitchell, "Application of UHF sensors in power system equipment for partial discharge detection: A review," *Sensors*, vol. 19, no. 5, p. 1029, Feb. 2019.
[4] M. Mondal and G. B. Kumbhar, "Partial discharge localization in a power transformer: Methods, trends, and future research," *IETE Tech. Rev.*, vol. 34, no. 5, pp. 504–513, Aug. 2016.
[5] Y. Sung, "Dual-band circularly polarized stack-ring antenna," *J. Electromagn. Eng. Sci.*, vol. 19, no. 1, pp. 37–41, Jan. 2019.
[6] Z. Zahid, L. Qu, H.-H. Kim, and H. Kim, "Circularly polarized loop-type ground radiation antenna for IoT applications," *J. Electromagn. Eng. Sci.*, vol. 19, no. 3, pp. 153–158, Jul. 2019.
[7] P. K. T. Rajanna, K. Rudramuni, and K. Kandasamy, "A wideband circularly polarized slot antenna backed by a frequency selective surface," *J. Electromagn. Eng. Sci.*, vol. 19, no. 3, pp. 166–171, Jul. 2019.
[8] M. Khosronejad and G. G. Gentili, "Design of an archimedean spiral UHF antenna for pulse monitoring application," in *Proc. Loughborough Antennas Propag. Conf. (LAPC)*, Loughborough, U.K., Nov. 2015, pp. 1–4.
[9] J. Lee, J. Cho, J. Choi, H. Choo, and K.-Y. Jung, "Design of a miniaturized spiral antenna for partial discharge detection system," *Microw. Opt. Technol. Lett.*, vol. 60, no. 1, pp. 75–78, Jan. 2018.
[10] H.-B. Kim, K.-C. Hwang, and H.-S. Kim, "Cavity-backed two-arm spiral antenna with a ring-shaped absorber for partial discharge diagnosis," *J. Electr. Eng. Technol.*, vol. 8, no. 4, pp. 856–862, Jul. 2013.
[11] X. Zhang, Y. Han, W. Li, and X. Duan, "A rectangular planar spiral antenna for GIS partial discharge detection," *Int. J. Antennas Propag.*, vol. 2014, pp. 1–7, May 2014.
[12] Y. Wang, J. Li, C. Li, B. Ouyang, and Z. Zheng, "A study on a miniaturized planar spiral antenna for partial discharge detection in GIS," *High Voltage Eng.*, vol. 22, Jan. 2016, Art. no. 02015.
[13] T. Li, M. Rong, C. Zheng, and X. Wang, "Development simulation and experiment study on UHF partial discharge sensor in GIS," *IEEE Trans. Dielectr. Electr. Insul.*, vol. 19, no. 4, pp. 1421–1430, Aug. 2012.
[14] Y. Wang, J. Wu, W. Chen, and Y. Wang, "Design of a UHF antenna for partial discharge detection of power equipment," *J. Sensors*, vol. 2014, pp. 1–8, Oct. 2014.
[15] L. Baby and N. R. Michael, "Self-complementary two arm Archimedean spiral antenna for aircraft applications," *Int. J. Current Eng. Technol.*, vol. 5, no. 5, pp. 3435–3438, Oct. 2015.
[16] C. A. Balanis, *Antenna Theory: Analysis and Design*, 3rd ed. Hoboken, NJ, USA: Wiley, 2005.
[17] H. Nakano, M. Ikeda, K. Hitosugi, and J. Yamauchi, "A spiral antenna sandwiched by dielectric layers," *IEEE Trans. Antennas Propag.*, vol. 52, no. 6, pp. 1417–1423, Jun. 2004.
[18] B. C. Wadell, *Transmission Line Design Handbook*. Norwood, MA, USA: Artech House, 1991.
[19] D. S. Woo, Y.-K. Cho, and K. W. Kim, "Balance analysis of microstrip-to-CPS baluns and its effects on broadband antenna performance," *Int. J. Antennas Propag.*, vol. 2013, pp. 1–9, Mar. 2013.

SEUNGYONG PARK received the B.S. degree from the School of Information and Communication Engineering, Chungbuk University, Cheongju, South Korea, in 2016. He is currently pursuing the Ph.D. degree in electrical engineering with Hanyang University, Seoul, South Korea. His current research interests include Doppler radar for medical application and antenna design for next generation wireless communication systems.

KYUNG-YOUNG JUNG (Senior Member, IEEE) received the B.S. and M.S. degrees in electrical engineering from Hanyang University, Seoul, South Korea, in 1996 and 1998, respectively, and the Ph.D. degree in electrical and computer engineering from The Ohio State University, Columbus, OH, USA, in 2008.

From 2008 to 2009, he was a Postdoctoral Researcher with The Ohio State University, and from 2009 to 2010, he was an Assistant Professor with the Department of Electrical and Computer Engineering, Ajou University, Suwon, South Korea. Since 2011, he has been working with Hanyang University, where he is currently an Associate Professor with the Department of Electronic Engineering. His current research interests include computational electromagnetics, bioelectromagnetics, and nanoelectromagnetics.

Dr. Jung was a recipient of the Graduate Study Abroad Scholarship from the National Research Foundation of Korea, the Presidential Fellowship from The Ohio State University, the Best Teacher Award from Hanyang University, and the Outstanding Research Award from the Korean Institute of Electromagnetic Engineering Society.